

Article

Identification and Biological Characterization of the Pyrazolo[3,4-*d*]pyrimidine Derivative SI388 Active as Src Inhibitor

Claudia Contadini ^{1,2,†}, Claudia Cirotti ^{1,2,†} , Anna Carbone ³, Mehrdad Norouzi ^{1,2}, Annarita Cianciusi ³, Emmanuele Crespan ⁴ , Cecilia Perini ⁴ , Giovanni Maga ⁴ , Daniela Barilà ^{1,2,*}, Francesca Musumeci ^{3,*}  and Silvia Schenone ³

¹ Laboratory of Cell Signaling, IRCCS-Fondazione Santa Lucia, 00179 Rome, Italy; claudiacontadini@gmail.com (C.C.); claudiacirotti89@gmail.com (C.C.)

² Department of Biology, University of Rome "Tor Vergata", 00133 Rome, Italy

³ Department of Pharmacy, University of Genoa, Viale Benedetto XV, 3, 16132 Genoa, Italy; annar.cianciusi@gmail.com (A.C.); schenone@difar.unige.it (S.S.)

⁴ Institute of Molecular Genetics (IGM), IGM-CNR, Via Abbiategrasso 207, 27100 Pavia, Italy; giovanni.maga@igm.cnr.it (G.M.)

* Correspondence: francesca.musumeci@unige.it (F.M.); daniela.barila@uniroma2.it (D.B.)

† These authors contributed equally to this work.

Abstract: Src is a non-receptor tyrosine kinase (TK) whose involvement in cancer, including glioblastoma (GBM), has been extensively demonstrated. In this context, we started from our *in-house* library of pyrazolo[3,4-*d*]pyrimidines that are active as Src and/or Bcr-Abl TK inhibitors and performed a lead optimization study to discover a new generation derivative that is suitable for Src kinase targeting. We synthesized a library of 19 compounds, **2a-s**. Among these, compound **2a** (SI388) was identified as the most potent Src inhibitor. Based on the cell-free results, we investigated the effect of SI388 in 2D and 3D GBM cellular models. Interestingly, SI388 significantly inhibits Src kinase, and therefore affects cell viability, tumorigenicity and enhances cancer cell sensitivity to ionizing radiation.

Keywords: Src kinase; glioblastoma; radiotherapy resistance; pyrazolo[3,4-*d*]pyrimidines



Citation: Contadini, C.; Cirotti, C.; Carbone, A.; Norouzi, M.; Cianciusi, A.; Crespan, E.; Perini, C.; Maga, G.; Barilà, D.; Musumeci, F.; et al. Identification and Biological Characterization of the Pyrazolo[3,4-*d*]pyrimidine Derivative SI388 Active as Src Inhibitor. *Pharmaceuticals* **2023**, *16*, 958. <https://doi.org/10.3390/ph16070958>

Academic Editor: Zaihui Zhang

Received: 26 May 2023

Revised: 27 June 2023

Accepted: 30 June 2023

Published: 4 July 2023



Copyright: © 2023 by the authors. Licensee MDPI, Basel, Switzerland. This article is an open access article distributed under the terms and conditions of the Creative Commons Attribution (CC BY) license (<https://creativecommons.org/licenses/by/4.0/>).

1. Introduction

Src is a non-receptor tyrosine kinase (TK) belonging to the Src family kinases (SFKs), which comprises different members, including Fyn. Src involvement in cancer has been extensively demonstrated; indeed, Src was the first TK and the first oncogene ever identified [1–3]. Several studies have shown Src kinase deregulation in different tumors; interestingly, Src hyperactivation is rarely due to mutations or gene duplication, while it is mainly linked to the aberrant activation of upstream receptor tyrosine kinases (RTKs) including EGFR, PDGFR, and MET. Src constitutive activation results in aberrant cell proliferation, survival, and migration and sustains angiogenesis, metastasis development, and resistance to therapy [4].

We previously developed a wide library of pyrazolo[3,4-*d*]pyrimidines active as Src, Fyn, and/or Bcr-Abl (another cytoplasmic TK) inhibitors. Many derivatives exhibited activity on different *in vitro* and *in vivo* tumor models characterized by a deregulation of the above mentioned kinases, such as osteosarcoma, chronic myelogenous leukemia (CML), neuroblastoma (NB), and glioblastoma (GBM) [5–9].

In several cases, the most active compounds were decorated with an anilino group at the C4 position. For instance, derivative **1a** (SI83) was active in a xenograft mouse model of osteosarcoma [9], compound **1b** (SI223) reduced more than 50% of the tumor volume in

mice inoculated with 32D-T315I CML cells [5], and compound **1c** (SI306) showed activity in in vivo models of NB and GBM [6,7] (Figure 1).

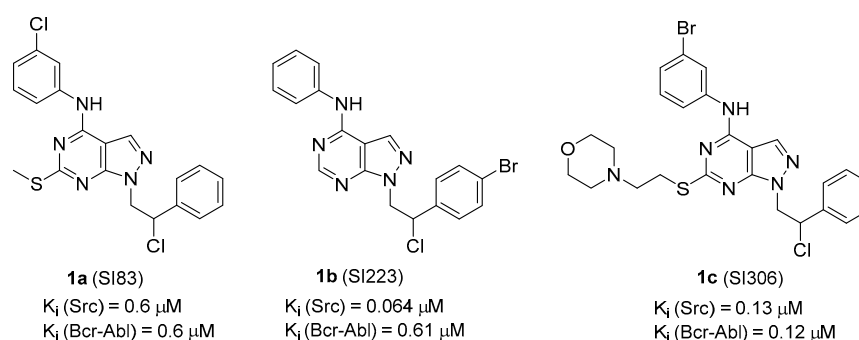
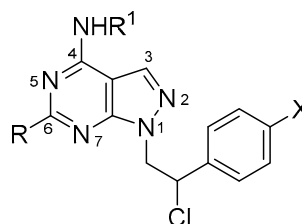


Figure 1. Structure and enzymatic activity of *in-house* 4-anilino-substituted pyrazolo[3,4-*d*]pyrimidines **1a–c**.

Starting from these data, we decided to synthesize a library of 19 compounds, **2a–s**, to extend the structure–activity relationship (SAR) of this class of inhibitors. Compounds **2a–s** (Table 1) were designed by partially combining the structural features of the lead compounds **1a–c** and evaluated in enzymatic assays against Src, Abl and Fyn, based on the activity of *in-house* pyrazolo[3,4-*d*]pyrimidines that were previously synthesized. Interestingly, this study led to the identification of **2a** (SI388), a quite potent Src inhibitor endowed with increased activity compared the lead compound **1a**.

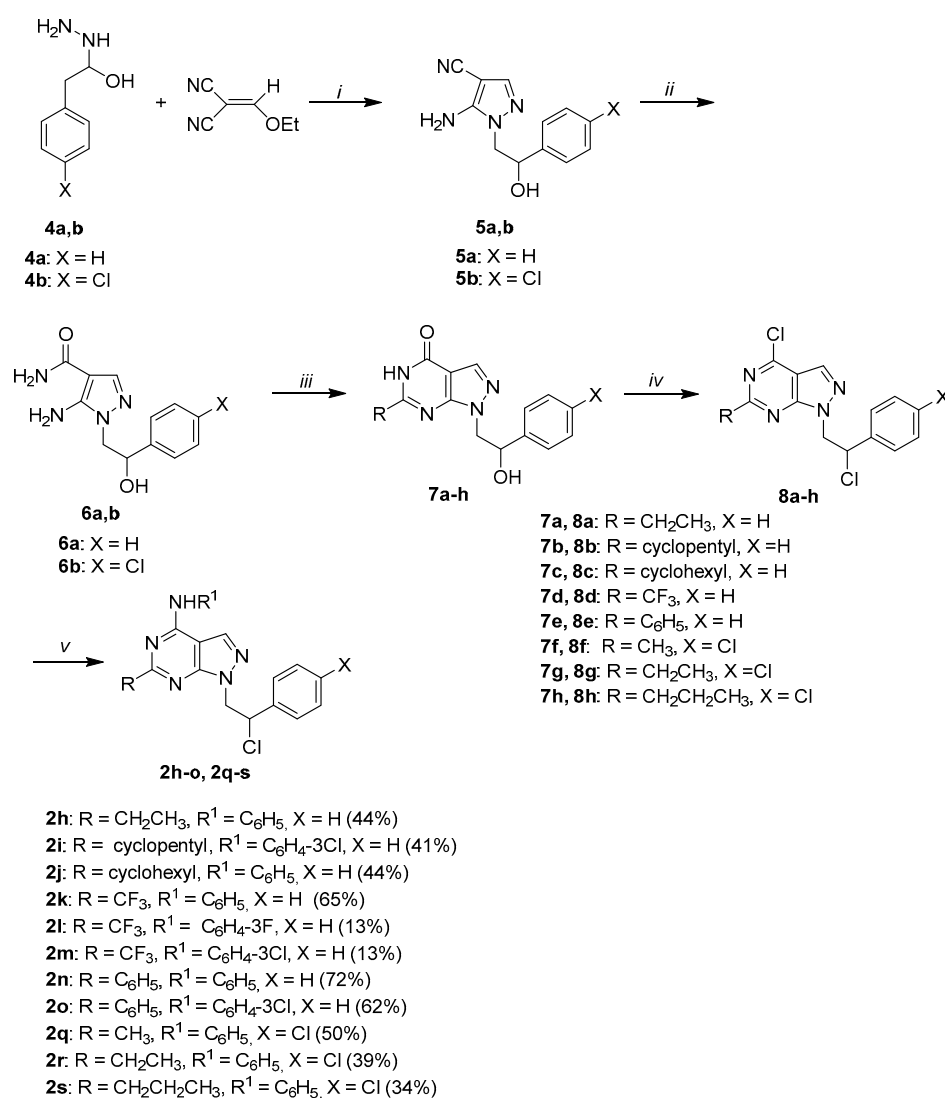
Table 1. Structure of compounds **2a–s**.



	R	R ¹	X
2a (SI388)	SCH ₃	C ₆ H ₄ -2Cl	H
2b	SCH ₃	C ₆ H ₄ -4Cl	H
2c	SCH ₂ CH ₃	C ₆ H ₅	H
2d	SCH(CH ₃) ₂	C ₆ H ₄ -3Cl	H
2e	SCH ₂ CH ₂ -4-morpholin-1-yl	C ₆ H ₄ -2Cl	H
2f	SCH ₂ CH ₂ -4-morpholin-1-yl · HCl	C ₆ H ₃ -3OH-4F	H
2g	SCH ₂ CH ₂ -4-morpholin-1-yl	C ₆ H ₂ -2F-4F-5OH	H
2h	CH ₂ CH ₃	C ₆ H ₅	H
2i	cyclopentyl	C ₆ H ₄ -3Cl	H
2j	cyclohexyl	C ₆ H ₅	H
2k	CF ₃	C ₆ H ₅	H
2l	CF ₃	C ₆ H ₄ -3F	H
2m	CF ₃	C ₆ H ₄ -3Cl	H
2n	C ₆ H ₅	C ₆ H ₅	H
2o	C ₆ H ₅	C ₆ H ₄ -3Cl	H
2p	SCH ₃	C ₆ H ₅	F
2q	CH ₃	C ₆ H ₅	Cl
2r	CH ₂ CH ₃	C ₆ H ₅	Cl
2s	CH ₂ CH ₂ CH ₃	C ₆ H ₅	Cl

Based on these cell-free results, we decided to investigate the effect of SI388 using 2D and 3D GBM cellular models in which Src activity has been previously reported to be aberrantly activated [10,11].

We provide evidence of the ability of SI388 to affect cell viability and tumorigenicity via Src inhibition. Furthermore, we demonstrate that SI388 increases cell sensitivity to ionizing radiation.



Scheme 2. Synthesis of compounds **2h-o** and **2q-s**. ^b **Reagents and conditions:** (i) abs EtOH, reflux, 6 h, 51.71%; (ii) 2M NaOH, abs EtOH, reflux, 2 h, 58.66%; (iii) appropriate alkyl ester, EtONa, abs EtOH, reflux, 6–12 h, 44–80%; (iv) POCl₃/DMF, CHCl₃, reflux, 6–12 h, 81–98%; (v) appropriate aniline, abs EtOH, reflux, 5 h (to obtain compounds **2h-j**, **2n,o**, and **2q-s**, 34–72%), or appropriate aniline, abs EtOH, MW, 80 °C, P_{atm}, 2–10 min (to obtain compounds **2k-m**, 13–65%).

We followed a different route for synthesizing C₆-alkyl derivatives (Scheme 2). The opportune 2-hydrazino-1-phenylethanol **4a,b** [9] was reacted with ethoxymethylene-malononitrile at reflux for 6 h affording the 5-amino-1-(2-hydroxy-2-phenylethyl)-1*H*-pyrazole-4-carbonitrile intermediates **5a,b**. Hydrolysis of the cyano groups of **5a,b** to the corresponding carboxamides afforded compounds **6a,b**. Cyclization of **6a,b** by treatment with the appropriated alkyl esters and sodium ethylate in ethanol at reflux gave the 1-(2-hydroxy-2-phenylethyl)-6-alkyl-1,5-dihydro-4*H*-pyrazolo[3,4-*d*]pyrimidin-4-ones **7a-h**. Treatment of **7a-h** with the Vilsmeier complex (POCl₃/DMF) in CHCl₃ at reflux led to the dichloro derivatives **8a-h**. Finally, these intermediates were reacted with the appropriate aniline, in accordance with the conditions described in Scheme 1, to obtain the desired compounds **2h-j**, **2n,o**, and **2q-s**. Otherwise, compounds **2k-m**, bearing a trifluoromethyl group at the C₆ position, were obtained by MW-assisted synthesis at 80 °C for 2–10 min in an open vessel.

2.2. Enzymatic Activity

Pyrazolo[3,4-*d*]pyrimidines **2a-s** were evaluated in enzymatic assays against Src, Bcr-Abl, and Fyn, using compound **1a** as the reference. The percentage of inhibition was

calculated at different concentrations (100, 10, and 1 μM) (Table S1, in the Supporting Information), and the K_i was determined for the most promising derivatives (Table 2).

Table 2. K_i towards Src, Fyn and Abl of compound **1a** (SI83) and derivatives **2a-s**.

	Src K_i (μM) ^a	Fyn K_i (μM) ^a	Bcr-Abl K_i (μM) ^a
1a (SI83)	0.6	N.D. ^b	0.6
2a (SI388)	0.423 \pm 0.093	0.419 \pm 0.075	0.45 \pm 0.29
2c	N.D.	N.D.	N.D.
2h	N.D.	10.27 \pm 3.13	N.D.
2k	N.D.	3.79 \pm 1.01	N.D.
2p	14.44 \pm 4.4	2.68 \pm 0.37	N.D.
2q	16.49 \pm 4	2.07 \pm 1.1	N.D.
2r	N.D.	1.74 \pm 0.71	N.D.
2s	N.D.	10.2 \pm 2.11	N.D.

^a The values were obtained from the mean of at least three experiments. ^b N.D. = Not Determined.

Interestingly, compound **2a**, possessing K_i values of 0.423 and 0.419 μM for Src and Abl, respectively, emerged as a valuable dual Src/Bcr-Abl inhibitor [9,16]. On the other hand, the corresponding para substituted derivative **2b** was inactive.

Unfortunately, other derivatives also generally showed low activity in cell-free assays. The introduction of an alkyl chain at C6 (compounds **2h-o** and **2q-s**) did not afford potent SFK/Bcr-Abl inhibitors. This SAR could be explained by the fact that alkyl groups cannot form polar interactions with the target and stabilize the complex. Furthermore, it is worth pointing out that the polar thioethylmorpholinyl chain (compounds **2e-g**) also did not lead to effective Src/Fyn/Bcr-Abl inhibitors. This result is quite unexpected since other sets of 6-thioethylmorpholinyl pyrazolo[3,4-*d*]pyrimidines recently published by us [12,13] showed an activity profile towards Src and/or Bcr-Abl in the nanomolar range. In this case, we can hypothesize that the activity loss is due to the different substituents on the anilino ring. A careful comparison of previous and current data allowed us to shed light on this behavior and expand our SAR knowledge. Many of the best in-house thioethylmorpholinyl derivatives that are active as Src inhibitors bear a 2-chloro-5-hydroxy anilino group at C4 [12]. Modeling studies highlighted that the OH was able to form a hydrogen bond with a residue of glutamate of the catalytic pocket of Src, enhancing the affinity between the kinase and the inhibitor [7]. The current study further confirmed these *in silico* results: compound **2e** was inactive towards all of the tested kinases, while its hydroxylated analog compound possessed a K_i value of 190 nM towards Src [12]. Furthermore, data reported in Table 1 show that introducing a fluorine atom in the ortho or ortho/para positions of the anilino ring (compounds **2f** and **2g**) led to inactive compounds. We already reported that a 2-fluoro-3-hydroxy anilino derivative was less active than the corresponding chloro analog compound [12]; in the study, we also demonstrated that moving the fluorine to the para position or the presence of two fluorine atoms did not lead to positive effects on the activity.

Overall, this study allowed us to identify a low micromolar Src/Bcr-Abl inhibitor (**2a**). Because in-house C6 substituted pyrazolo-pyrimidines generally showed activity in tumors characterized by Src overexpression, we decided to investigate the activity of **2a** in GBM cellular models.

2.3. Cell Biology

2.3.1. SI388 Inhibits Src Kinase Activity in GBM Cellular Models

To test the ability of compound **2a** (SI388) to inhibit Src activity *in vitro*, we took advantage of glioblastoma cellular models. Glioblastoma, indeed, was the first cancer type to be systematically studied by The Cancer Genome Atlas Research Network (TCGA)[17], who identified the RTK/Ras/PI3K pathway as having the most frequently deregulated signaling [4,18], with Src being a common node downstream of different RTKs [4,10].

U251 and T98G glioblastoma cell lines were treated with two ascending drug concentrations (10 nM and 1 μ M) or DMSO for 24 h and Src activity was revealed by immunoblotting with a specific anti-phospho Tyr416-Src (anti-pY416Src) antibody. As shown in Figure 2 (panels A and B), we observed a reduction in Src phosphorylation on Tyr416 (Y416) after treatment with 2a in a dose-dependent manner. Similar results were also obtained upon treatment with 1a (SI383) (Figure 2, panels C and D), its analogue compound, and dasatinib (DAS) (Figure 2, panels E and F), a well-known commercially available Src inhibitor.

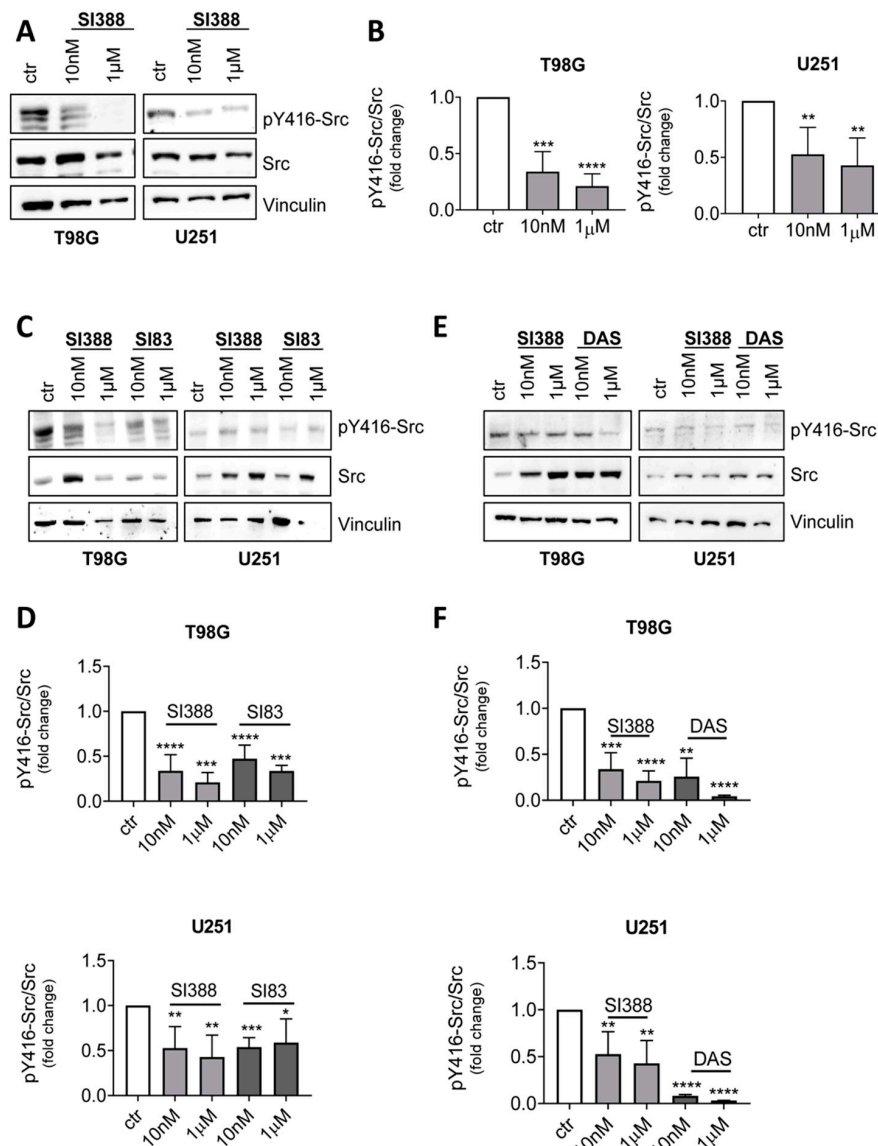


Figure 2. SI388 inhibits Src activity in T98G and U251 cell lines. (A,B) Western blot analysis (A) and relative quantification (B) of pY416-Src in T98G and U251 cell lines treated with SI388 10 nM and 1 μ M for 24 h. Vinculin was used as loading control. (C,D) Western blot analysis (C) and relative quantification (D) of pY416-Src in T98G and U251 cell lines treated with SI388 or SI83 at two different concentrations for 24 h. Vinculin was used as loading control. (E,F) Western blot analysis (E) and relative quantification (F) of pY416-Src in T98G and U251 cell lines treated with SI388 or dasatinib (DAS) at two different concentrations for 24 h. Vinculin was used as loading control. Histograms summarize quantitative data of the mean \pm S.E.M. of four independent experiments. Statistical analyses: unpaired Student's *t*-test: * $p < 0.05$; ** $p < 0.01$; *** $p < 0.001$; **** $p < 0.0001$.

2.3.2. SI388 Reduces Cell Growth and Viability in GBM Cell Lines

To further characterize the ability of SI388 to inhibit tumor growth, we performed clonogenic assays using T98G and U251 cell lines. Cells were starved and treated for 24 h with increasing concentration (10 nM, 1 μ M, and 25 μ M) of SI388 or DAS. The ability of single cells to proliferate and produce colonies was evaluated after 15 days, both in control conditions (treated with DMSO) and after treatment with different Src inhibitors. As shown in Figure 3 (panels A and B), both SI388 and DAS impaired cell growth and proliferation in a dose-dependent manner in both cell lines.

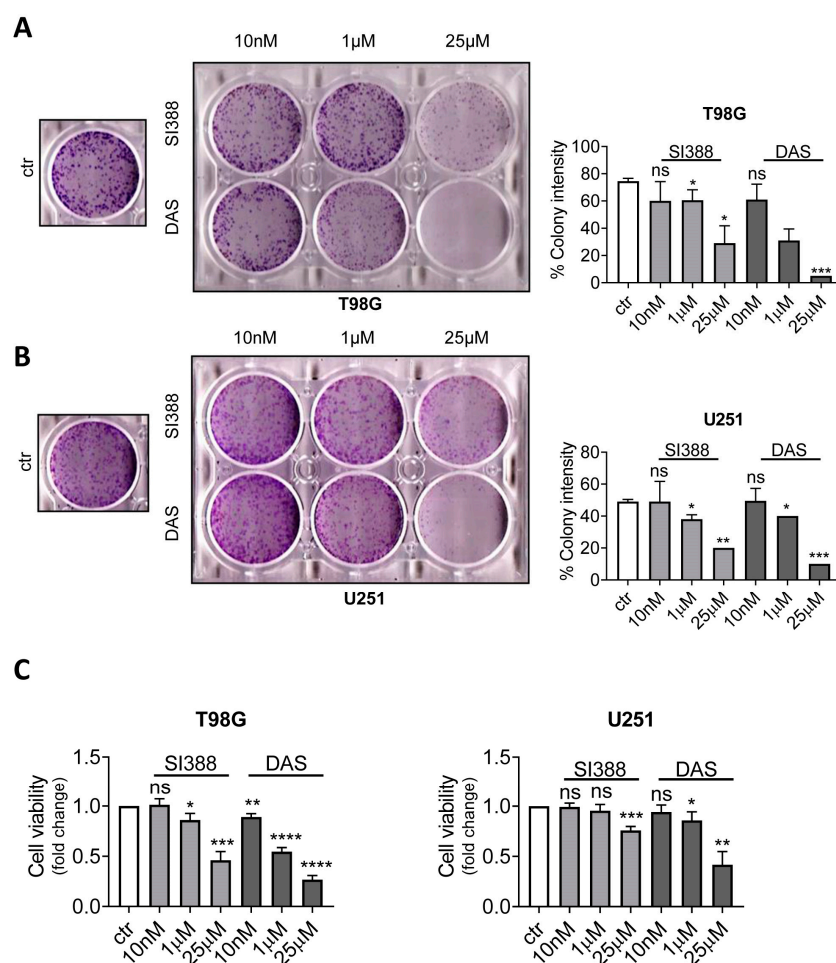


Figure 3. SI388 inhibits cell proliferation and viability. (A,B) Representative image (left) and relative quantification (right) of clonogenic assays performed on T98G and U251 cell lines treated with ascending concentrations of SI388 or dasatinib (DAS) for 24 h. DMSO was used as control. (C) Histogram representing the percentage of cell viability evaluated by MTS assay on T98G and U251 cell lines treated as in A for 72 h. Histograms summarize quantitative data of the mean \pm S.E.M of three independent experiments. Statistical analyses: unpaired Student's *t*-test: * $p < 0.05$; ** $p < 0.01$; *** $p < 0.001$; **** $p < 0.0001$; ns, not significant.

Next, the ability of SI388 to inhibit cell viability was evaluated using an MTS assay. As shown in Figure 3C, SI388 significantly impaired cell viability after 72 h of drug treatment in a dose-dependent manner both in T98G and in U251 cells.

2.3.3. SI388 Inhibits Src Kinase Activity in GBM Patient-Derived Cancer Stem Cells and Reduces Their Ability to form Neurospheres

Recently, gene expression subtyping highlighted that the mesenchymal GBM subtype shows higher Src pathway activation, resulting in enhanced sensitivity to dasatinib treatment compared to other GBM subtypes [19].

For this reason, we next evaluated the ability of SI388 to affect cell growth in a patient-derived mesenchymal GBM cancer stem cells, named GBMSC83, cultured in non-adherent conditions to form neurospheres.

Firstly, we observed a significant reduction in phosphorylation of Src on Tyr416 upon a 1 μ M SI388 treatment in this system; although, the inhibitory effect of SI388 is weaker compared to a 1 μ M DAS treatment (Figure 4A). We then demonstrated that both treatments significantly decreased the growth of spheres, resulting in an overall reduced diameter of the spheres compared to the control condition (Figure 4B) and a reduced average number of cells per sphere (Figure 4C).

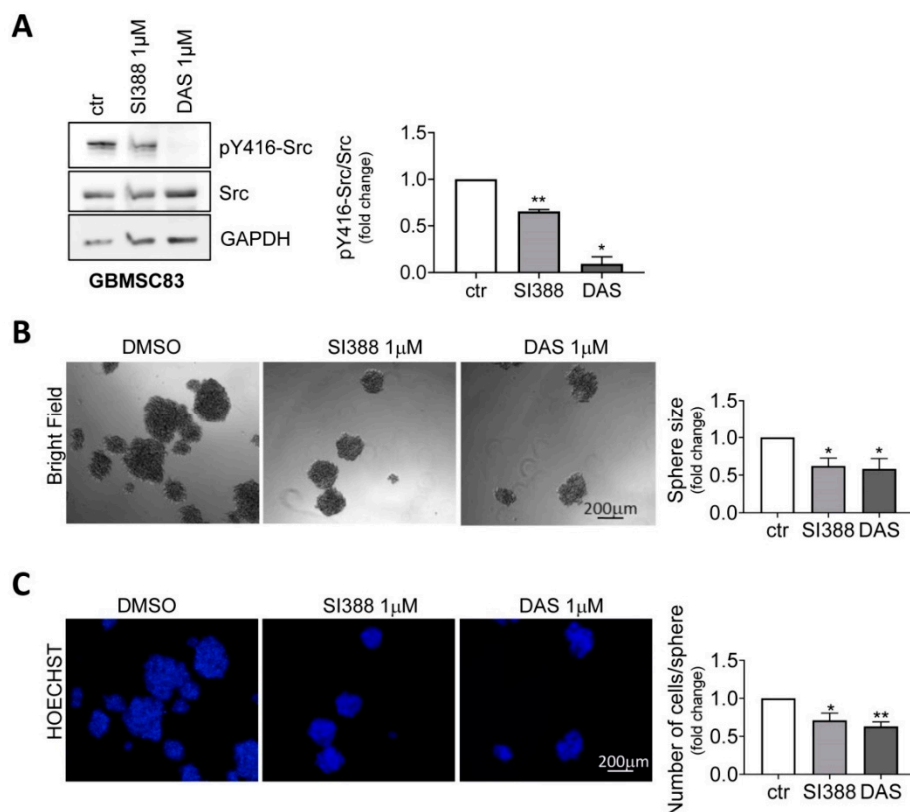


Figure 4. SI388 inhibits Src activity in GBM stem cells and affects neurosphere size. (A) Western blot analysis (left) and relative quantification (right) of pY416-Src in GBMSC83 cells treated with SI388 (1 μ M) or dasatinib (DAS 1 μ M) for 24 h. GAPDH was used as loading control. (B,C) Neurosphere assay analysis on GBMSC83 cells treated with SI388 1 μ M or dasatinib (DAS) 1 μ M for 72 h. (B) Brightfield images and histogram of mean neurosphere diameter (reported as fold change to control). (C) Hoechst staining and histogram of the number of cells per sphere (fold change to control). Histograms summarize quantitative data of the mean \pm S.E.M. of three independent experiments. Statistical analyses: paired Student's *t*-test: * $p < 0.05$; ** $p < 0.01$.

2.3.4. SI388 Increases Cell Sensitivity to Ionizing Radiation (IR) Treatment

To further strengthen our findings, we next investigated if SI388 treatment could increase cell sensitivity to radiotherapy of GBM cells.

To this aim, T98G and U251 cells were pre-incubated or not with SI388 for 24 h and then irradiated (10 Gy). MTS assays revealed that SI388 pre-treatment increases the sensitivity to IR in both GBM cell lines; although, this result was only statistically significant in T98G cells (Figure 5A).

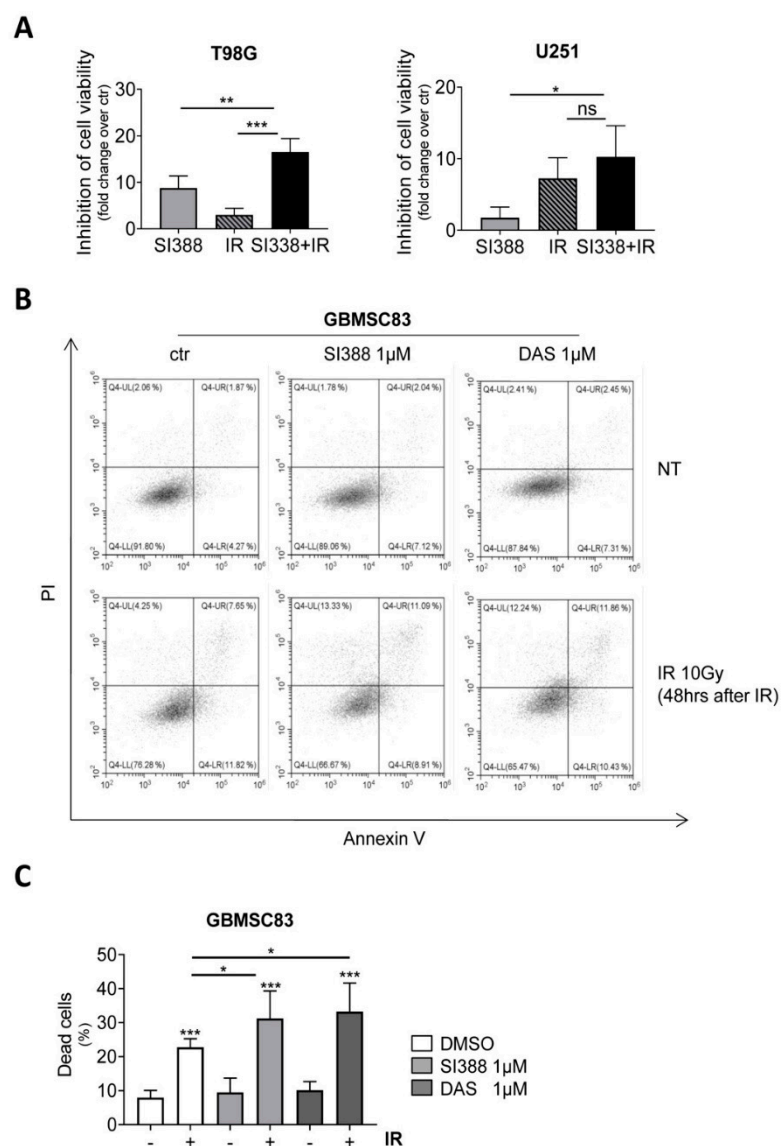


Figure 5. SI388 increases cell sensitivity to IR. (A) Histogram representing the percentage of the inhibition of cell viability evaluated by MTS assays after 48 h from IR (10Gy) on T98G and U251 cell lines with or without SI388 (1 μ M). (B,C) Cytofluorimetric analysis of AnnexinV-PI (B) and relative histogram (C) showing percentage of dead GBMSC83 cells after 48 h from IR 10 Gy with or without SI388 (1 μ M) or dasatinib (DAS, 1 μ M). Histograms summarize quantitative data of the mean \pm S.E.M. of four independent experiments. Statistical analyses: unpaired Student's *t*-test: * $p < 0.05$; ** $p < 0.01$; *** $p < 0.001$; ns, not significant.

GBMSC83 cells were pretreated with 1 μ M SI388 or 1 μ M DAS, or DMSO as a control, for 24 h and then irradiated (10 Gy). After 48 h from IR, cytofluorimetric analysis of AnnexinV-PI staining was performed. Interestingly, SI388, as well as dasatinib, sensitized cells to IR and significantly increased the percentage of cell death compared to the control samples (Figure 5, panels B and C).

3. Materials and Methods

3.1. Chemistry

All commercially available chemicals were used as purchased. DCM was dried over calcium hydride. Anhydrous reactions were run under a positive pressure of dry N_2 or argon. TLC was carried out using Merck TLC plates silica gel 60 F254. Chromatographic purifications were performed on columns packed with Merck 60 silica gel, 23–400 mesh,

for flash technique. ^1H NMR and ^{13}C NMR spectra were recorded on a Bruker Avance DPX400 (at 400 MHz for ^1H and 100 MHz for ^{13}C) or using a Varian Gemini 200 (200 MHz for ^1H) in DMSO- d_6 , CDCl_3 , or acetone- d_6 as solvents as indicated. Chemical shifts (δ) were expressed in parts per million (ppm) relative to tetramethylsilane (TMS), which was used as the internal standard. Data are shown as follows: chemical shift, multiplicity (s = singlet, d = doublet, t = triplet, q = quartet, quint = quintet, sx = sextet, dd = doublet of doublets, tt = triple of triplets, bs = broad singlet), coupling constant (J) in Hertz (Hz), and integration. Elemental analysis for C, H, N, and S was determined using Thermo Scientific Flash 2000 and results were within $\pm 0.4\%$ of the theoretical value. All target compounds possessed a purity of $\geq 95\%$, which was verified by elemental analysis. Microwave irradiation experiments were conducted using a CEM Discover synthesis unit (CEM Corp., Matthews, NC, USA). The machine consists of a continuous focused microwave power delivery system with operator selectable power output from 0 to 300 W. The temperature of the contents of the vessels was monitored using a calibrate infrared temperature control mounted under the reaction vessel. All of the experiments were performed using a stirring option whereby the contents of the vessel are stirred by means of a rotating magnetic plate located below the floor of the microwave cavity and a Teflon-coated magnetic stir bar in the vessel.

Synthesis of the intermediates **3a** [9], **3b** [15], **3c** [14], **3d** [8], **3e** and **4a,b** [9] has already been reported by us.

3.1.1. General Procedure for the Synthesis of Final Compounds **2a-e**, **2h-j** and **2n-s**

A solution of the appropriate 4-chloro derivatives **3a-e**, **8a-c**, or **8e-h** (1 mmol) and the appropriate aniline (2 mmol) in absolute ethanol was refluxed for 5 h. After cooling, the solvent was evaporated under reduced pressure, and the crude was treated with water (20 mL), and then extracted with CH_2Cl_2 (20 mL). The organic phase was washed with water (20 mL), dried (MgSO_4), and concentrated under reduced pressure. The obtained oil was crystallized by adding a mixture of diethyl ether/petroleum ether (bp 40–60 °C) (1:1) and standing in a refrigerator to afford a white solid, which was recrystallized from absolute ethanol.

1-(2-Chloro-2-phenylethyl)-*N*-(2-chlorophenyl)-6-(methylthio)-1*H*-pyrazolo[3,4-*d*]pyrimidin-4-amine **2a** (SI388). Yield: 69% (white solid). Mp: 169–171 °C. ^1H NMR (400 MHz, DMSO- d_6): δ 10.02 (s, 1H), 7.67 (br s, 1H), 7.58–7.56 (m, 2H), 7.49–7.47 (m, 2H), 7.41–7.30 (m, 5H), 5.64–5.60 (m, 1H), 4.89–4.83 and 4.76–4.71 (2m, 2H), 2.40 (s, 3H). ^{13}C NMR (101 MHz, DMSO- d_6): δ 169.67, 155.07, 153.98, 137.98, 134.71, 132.21, 131.67, 129.87, 129.09, 128.79, 127.79, 127.44, 126.41, 125.01, 98.57, 60.10, 53.78, 14.37. IR (KBr disc) cm^{-1} : 3156 (NH). Elem. anal. calcd. for $\text{C}_{20}\text{H}_{17}\text{N}_5\text{Cl}_2\text{S}$: C 55.82, H 3.98, N 16.27, S 7.45; found: C 55.78, H 4.11, N 16.45, S 7.07.

1-(2-Chloro-2-phenylethyl)-*N*-(4-chlorophenyl)-6-(methylthio)-1*H*-pyrazolo[3,4-*d*]pyrimidin-4-amine **2b**. Yield: 71% (white solid). Analytical and spectroscopic data are in accordance with those previously reported by us [20].

1-(2-Chloro-2-phenylethyl)-6-(ethylthio)-*N*-phenyl-1*H*-pyrazolo[3,4-*d*]pyrimidin-4-amine **2c**. Yield: 51% (white solid). Mp: 128–131 °C. ^1H NMR (400 MHz, CDCl_3): δ 9.37 (br s, 1H), 7.49–7.40, 7.38–7.35 and 7.34–7.30 (3m, 11 H), 6.94 (br s, 1H), 5.43–5.40 (m, 1H), 4.87–4.81 and 4.71–4.44 (2m, 2H), 3.28–3.19 (q, 2H, $J = 8.0$ Hz), 1.46 (t, 3H, $J = 8.0$ Hz). ^{13}C NMR (101 MHz, CDCl_3): δ 153.98, 137.68, 136.15, 134.31, 130.01, 129.69, 129.37, 129.27, 128.90, 128.86, 127.48, 127.43, 127.31, 60.08, 53.83, 25.65, 14.25. IR (KBr disc) cm^{-1} : 3357 (NH). Elem. anal. calcd. for $\text{C}_{21}\text{H}_{20}\text{N}_5\text{ClS}$: C 61.53, H 4.92, N 17.08, S 7.82; found: C 61.31, H 4.66, N 17.23, S 8.02.

1-(2-Chloro-2-phenylethyl)-*N*-(3-chlorophenyl)-6-(isopropylthio)-1*H*-pyrazolo[3,4-*d*]pyrimidin-4-amine **2d**. Yield: 65% (white solid). Analytical and spectroscopic data are in accordance with those previously reported by us [20].

1-(2-Chloro-2-phenylethyl)-*N*-(2-chlorophenyl)-6-((2-morpholinoethyl)thio)-1*H*-pyrazolo[3,4-*d*]pyrimidin-4-amine **2e**. Yield: 62% (white solid). Mp: 117–118 °C. ^1H NMR (400 MHz, CDCl_3): δ 8.04 (br s, 1H), 7.52–7.46 (m, 3H), 7.37–7.32 (m, 6 H), 5.50–5.46 (m, 1H),

5.28–5.15 (m, 1H), 4.76–4.71 (m, 2H), 3.87 (br s, 4H), 3.37 (br s, 2H), 2.77 (br s, 6H). ^{13}C NMR (101 MHz, CDCl_3): δ 162.52, 154.67, 154.45, 137.71, 137.52, 137.35, 135.78, 134.10, 133.84, 133.37, 129.41, 129.02, 127.43, 126.54, 110.80, 66.20, 60.87, 57.28, 54.24, 53.15, 31.46. IR (KBr disc) cm^{-1} : 3061 (NH). Elem. anal. calcd. for $\text{C}_{25}\text{H}_{26}\text{N}_6\text{OSCl}_2$: C 56.71, H 4.95, N 15.87, S 6.56; found: C 56.41, H 4.71, N 15.87, S 6.87.

1-(2-Chloro-2-phenylethyl)-6-ethyl-*N*-phenyl-1*H*-pyrazolo[3,4-*d*]pyrimidin-4-amine **2h**. Yield: 44% (white solid). Mp: 174–176 °C. ^1H NMR (400 MHz, DMSO-d_6): δ 9.92 (s, 1H), 8.17 (br s, 1H), 7.85 (d, 2H, $J = 7.6$ Hz), 7.47 (dd, 2H, $J = 8.0$ Hz, $J = 1.6$ Hz), 7.35–7.30 (m, 5H), 7.05 (t, 1H, $J = 7.2$ Hz), 5.67–5.63 (m, 1H), 4.96–4.90 and 4.79–4.72 (2m, 2H), 2.75 (q, 2H, $J = 7.6$ Hz), 1.27 (t, 3H, $J = 7.6$ Hz). ^{13}C NMR (400 MHz, DMSO-d_6): δ 169.29, 155.14, 154.56, 139.92, 138.51, 132.72, 129.47, 129.23, 129.18, 128.12, 123.66, 121.42, 99.70, 61.04, 52.96, 32.72, 13.13. IR (KBr disc) cm^{-1} : 3155 (NH). Elem. anal. calcd. for $\text{C}_{21}\text{H}_{20}\text{N}_5\text{Cl}$: C 66.75, H 5.33, N 18.53; found: C 66.92, H 5.41, N 18.64.

1-(2-Chloro-2-phenylethyl)-*N*-(3-chlorophenyl)-6-cyclopentyl-1*H*-pyrazolo[3,4-*d*]pyrimidin-4-amine **2i**. Yield: 41% (white solid). Mp: 189–190 °C. ^1H (400 MHz, DMSO-d_6): δ 10.08 (s, 1H), 8.33 (t, 1H, $J = 2.0$ Hz), 7.63 (dd, 1H, $J = 8.4$ Hz, $J = 1.2$ Hz), 7.46 (dd, 2H, $J = 8.0$ Hz, $J = 1.6$ Hz), 7.37–7.28 (m, 4H), 7.07 (dd, 1H, $J = 7.2$ Hz, $J = 1.2$ Hz), 5.66–5.63 (m, 1H), 4.95–4.90 and 4.82–4.77 (2m 2H), 3.21 (quint, 1H, $J = 8.0$ Hz), 2.02–1.96, 1.93–1.82, 1.79–1.78 and 1.65–1.62 (4m, 8H). ^{13}C NMR (101 MHz, DMSO-d_6): δ 171.91, 154.96, 154.25, 141.57, 138.45, 133.51, 132.61, 130.77, 129.46, 129.16, 128.10, 122.87, 120.44, 118.92, 99.94, 60.97, 52.96, 48.56, 33.06, 32.91, 26.39. IR (KBr disc) cm^{-1} : 3068 (NH). Elem. anal. calcd. For $\text{C}_{24}\text{H}_{23}\text{N}_5\text{Cl}_2$: C 63.72, H 5.12, N 15.48; found: C 63.48, H 5.34, N 15.61.

1-(2-Chloro-2-phenylethyl)-6-cyclohexyl-*N*-phenyl-1*H*-pyrazolo[3,4-*d*]pyrimidin-4-amine **2j**. Yield: 44% (white solid). Mp: 134–136 °C. ^1H NMR (400 MHz, CDCl_3): δ 7.46–7.45 (m, 4H), 7.40–7.36 (m, 4H), 7.32–7.26 (m, 3H), 7.03 (br s, 1H), 5.48–5.45 (m, 1H), 4.92–4.87 and 4.82–4.77 (2m, 2H), 2.79 (tt, 1H, $J = 12.0$ Hz, $J = 3.6$ Hz), 2.04–2.01 (m, 2H), 1.89–1.86 (m, 2H), 1.77–1.65 (m, 3H), 1.47–1.31 (m, 3H). ^{13}C NMR (101 MHz, CDCl_3): δ 205.15, 154.56, 137.78, 133.40, 129.88, 129.59, 129.10, 128.77, 128.73, 127.49, 125.28, 98.09, 60.04, 53.66, 47.08, 46.23, 39.33, 31.53, 26.10, 25.97. IR (KBr disc) cm^{-1} : 3361 (NH). Elem. anal. calcd. For $\text{C}_{25}\text{H}_{26}\text{N}_5\text{Cl}$: C 69.51, H 16.21, N 6.07; found: C 69.72, H 15.82, N 15.87.

1-(2-Chloro-2-phenylethyl)-*N*,6-diphenyl-1*H*-pyrazolo[3,4-*d*]pyrimidin-4-amine **2n**. Yield: 72% (white solid). Mp: 130–140 °C (dec). ^1H NMR (400 MHz, CDCl_3): δ 8.52–8.50 (m, 2H), 7.54–7.43 (m, 10H), 7.38–7.26 (m, 4H), 5.55–5.52 (m, 1H), 5.04–4.98 and 4.89–4.84 (2m 2H). ^{13}C NMR (101 MHz, CDCl_3): δ 170.71, 170.09, 155.20, 145.56, 139.95, 135.55, 129.47, 129.01, 128.87, 128.85, 128.00, 127.53, 126.57, 126.37, 121.84, 117.02, 114.39, 59.58, 53.41. IR (KBr disc) cm^{-1} : 3347 (NH). Elem. anal. calcd. For $\text{C}_{25}\text{H}_{20}\text{N}_5\text{Cl}$: C 70.50, H 4.73, N 16.44; found: C 70.63, H 4.89, N 16.43.

1-(2-Chloro-2-phenylethyl)-*N*-(3-chlorophenyl)-6-phenyl-1*H*-pyrazolo[3,4-*d*]pyrimidin-4-amine **2o**. Yield: 62% (white solid). Mp: 82–84 °C. ^1H NMR (400 MHz, DMSO-d_6): δ 10.26 (s, 1H), 8.43–8.40 (m, 2H), 8.31 (s, 1H), 8.25 (t, 1H, $J = 2.0$ Hz), 7.77–7.74 (m, 1H), 7.55–7.50 (m, 5H), 7.43 (t, 1H, $J = 8.0$ Hz), 7.35–7.25 (m, 3H), 7.16–7.14 (m, 1H), 5.73–5.70 (m, 1H), 5.09–5.06 and 4.9489–4.88 (2m 2H). ^{13}C NMR (101 MHz, DMSO-d_6): δ 161.19, 155.27, 154.29, 141.27, 138.51, 138.26, 133.55, 132.94, 131.27, 130.99, 129.51, 129.19, 129.08, 128.69, 128.19, 123.30, 120.88, 119.46, 100.40, 61.09, 53.14. IR (KBr disc) cm^{-1} : 3291 (NH). Elem. anal. calcd. For $\text{C}_{25}\text{H}_{19}\text{N}_5\text{Cl}_2$: C 65.22, H 4.16, N 15.21; found: C 65.36, H 4.42, N 14.97.

1-(2-Chloro-2-(4-fluorophenyl)ethyl)-6-(methylthio)-*N*-phenyl-1*H*-pyrazolo[3,4-*d*]pyrimidin-4-amine **2p**. Yield: 47% (white solid). Mp: 227–230 °C. ^1H NMR (400 MHz, DMSO-d_6): δ 10.27 (s, 1H), 8.26 (br s, 1H), 7.78 (d, 2H, $J = 8.0$ Hz), 7.54–7.51 (m, 2H), 7.34 (t, 2H, $J = 7.6$ Hz), 7.17–7.13 (m, 2H), 7.09–7.06 (m, 1H), 5.67–5.63 (m, 1H), 4.90–4.84 and 4.77–4.72 (2m, 2H), 2.50 (s, 3H). ^{13}C NMR (101 MHz, DMSO-d_6): δ 169.17, 163.88, 161.44, 158.93, 154.61, 139.35, 134.88, 134.85, 133.55, 130.49, 130.41, 129.21, 116.14, 115.92, 99.03, 60.06, 53.06, 14.26. IR (KBr disc) cm^{-1} : 3093 (NH). Elem. anal. calcd. For: C 58.04, H 4.14, N 16.92, S 7.75; found: C 58.09, H 4.07, N 15.75, S 8.33.

1-(2-Chloro-2-(4-chlorophenyl)ethyl)-6-methyl-*N*-phenyl-1*H*-pyrazolo[3,4-*d*]pyrimidin-4-amine **2q**. Yield: 50% (white solid). Mp: 202–203 °C. ¹H NMR (400 MHz, DMSO-*d*₆): δ 9.92 (s, 1H), 8.14 (br s, 1H), 7.82 (d, 2H, *J* = 8.0 Hz), 7.52–7.49 (m, 2H), 7.41–7.33 (m, 4H), 7.06 (t, 2H, *J* = 7.6 Hz), 5.67–5.64 (m, 1H), 4.95–4.89 and 4.76–4.71 (2m, 2H), 2.48 (s, 3H). ¹³C NMR (101 MHz, DMSO-*d*₆): δ 165.25, 155.19, 154.52, 139.81, 137.61, 134.02, 132.80, 130.15, 129.26, 129.18, 123.87, 121.54, 99.48, 60.02, 52.80, 26.62. IR (KBr disc) cm⁻¹: 3153 (NH). Elem. anal. calcd. For C₂₀H₁₇N₅Cl₂: C 60.31, H 4.30, N 17.58; found: C 60.51, H 4.60, N 17.40.

1-(2-Chloro-2-(4-chlorophenyl)ethyl)-6-ethyl-*N*-phenyl-1*H*-pyrazolo[3,4-*d*]pyrimidin-4-amine **2r**. Yield: 39% (white solid). Mp: 193–195 °C. ¹H NMR (400 MHz, CDCl₃): δ 7.68 (s, 1H), 7.54–7.45 (m, 4H), 7.42–7.40 (m, 2H), 7.41–7.38 (m, 2H), 7.35–7.30 (m, 5H), 5.38–5.34 (m, 1H), 4.90–4.84 and 4.76–4.69 (2m, 2H), 2.99 (q, 2H, *J* = 7.6 Hz), 1.45 (t, 3H, *J* = 7.6 Hz). ¹³C NMR (101 MHz, CDCl₃): δ 155.56, 155.19, 137.42, 136.51, 134.86, 132.94, 129.76, 128.93, 128.92, 127.16, 125.25, 98.28, 59.10, 53.39, 40.77, 21.76, 14.01. IR (KBr disc) cm⁻¹: 3148 (NH). Elem. anal. calcd. For C₂₁H₁₉N₅Cl₂: C 61.17, H 4.64, N 16.99; found: C 61.48, H 4.77, N 16.65.

1-(2-Chloro-2-(4-chlorophenyl)ethyl)-*N*-phenyl-6-propyl-1*H*-pyrazolo[3,4-*d*]pyrimidin-4-amine **2s**. Yield: 34% (white solid). Mp: 154–156 °C. ¹H NMR (400 MHz, CDCl₃): δ 7.68 (br s, 1H), 7.54–7.51 (m, 4H), 7.42–7.40 (m, 2H), 7.34–7.27 (m, 4H), 5.39–5.35 (m, 1H), 4.89–4.81 and 4.74–4.69 (2m, 2H), 2.90 (t, 2H, *J* = 7.6 Hz), 1.94 (sx, 2H, *J* = 7.6 Hz), 1.05 (t, 2H, *J* = 7.6 Hz). ¹³C NMR (101 MHz, CDCl₃): δ 136.35, 135.95, 135.24, 133.55, 130.35, 129.60, 129.13, 128.95, 128.89, 128.82, 126.40, 58.98, 53.67, 40.90, 38.13, 21.47, 21.05, 13.77. IR (KBr disc) cm⁻¹: 3161 (NH). Elem. anal. calcd. For C₂₂H₂₁N₅Cl₂: C 61.98, H 4.96, N 16.43; found: C 62.14, H 5.04, N 16.49.

3.1.2. General Procedure for the Synthesis of Final Compounds **2f,g**

The appropriate 3-aminophenol derivative (5 mmol) was added to a solution of 4-chloro-1-(2-chloro-2-phenylethyl)-6-[(2-morpholinoethyl)thio]-1*H*-pyrazolo[3,4-*d*]pyrimidine **3d** (1 mmol, 438 mg) in absolute ethanol (10 mL), and the mixture was refluxed for 3–5 h. After cooling to room temperature, the solvent was evaporated under reduced pressure and the crude was solved in ethyl acetate (10 mL), washed with 0.1 N HCl solution (2 × 10 mL), 1 N NaOH solution (10 mL) and brine (2 × 10 mL), dried (MgSO₄), filtered, and concentrated under reduced pressure to give a brown oil which crystallized by adding a 1:1 mixture of diethyl ether/petroleum ether (bp 40–60 °C) affording yellow solid.

5-((1-(2-Chloro-2-phenylethyl)-6-[(2-morpholinoethyl)thio]-1*H*-pyrazolo[3,4-*d*]pyrimidin-4-yl)amino)-2-fluorophenol hydrochloride **2f**. Yield: 38% (yellow solid). Mp: 238–239 °C. ¹H NMR (200 MHz, DMSO-*d*₆): δ 10.23 (s, 1H), 10.18 (br s, 1H), 7.63–7.61, 7.41–7.39, and 7.19–7.15 (3m, 9H), 5.68–5.62 (m, 1H), 5.21–5.07 and 4.83–4.78 (2m, 2H), 3.89–3.18 (m, 12H). ¹³C NMR (50 MHz, DMSO-*d*₆): δ 167.84, 156.93, 152.04, 151.75, 150.39, 138.70, 138.23, 134.50, 129.39, 128.86, 127.54, 117.51, 113.09, 107.78, 106.14, 66.74, 61.80, 54.23, 52.66, 45.49, 31.87. IR (KBr disc) cm⁻¹: 3300–3100 (OH and NH). (NH). Elem. anal. calcd. For C₂₅H₂₇N₆O₂SCl₂F: C 53.10, H 4.81, N 14.26, S 5.67; found: C 53.25, H 4.77, N 14.49, S 5.27.

5-((1-(2-Chloro-2-phenylethyl)-6-((2-morpholinoethyl)thio)-1*H*-pyrazolo[3,4-*d*]pyrimidin-4-yl)amino)-2,4-difluorophenol **2g**. Yield: 25% (yellow solid). Mp: 146–149 °C. ¹H NMR (400 MHz, CDCl₃): δ 8.33 (br s, 1H), 7.89 (br s, 1H), 7.47–7.46 (m, 2H), 7.28–7.27 (m, 4H), 6.98–6.96 (m, 1H), 6.98–6.92 (m, 1H), 5.56–5.52 (m, 1H), 4.99–4.92 and 4.753–4.69 (2m, 2H), 3.92–3.91 (br s, 4H), 3.42 (br s, 2H), 3.98 (br s, 2H), 3.73 (br s, 4H). ¹³C NMR (101 MHz, CDCl₃) δ 168.21, 157.49, 151.95, 151.03, 148.20, 146.02, 138.23, 134.50, 132.47, 129.39, 128.86, 127.54, 109.07, 106.92, 105.42, 66.82, 61.80, 54.23, 53.16, 51.43, 31.44. IR (KBr disc) cm⁻¹: 3420–3300 (OH and NH). Elem. anal. calcd. For C₂₅H₂₅N₆O₂SClF₂: C 54.89, H 4.61, N 15.36, S 5.86; found: C 55.00, H 4.70, N 15.47, S 5.67.

3.1.3. General Procedure for the Synthesis of Final Compounds **2k-m**

The opportune amine (2.1 mmol) was added to a solution of 4-chloro-1-(2-chloro-2-phenylethyl)-6-(trifluoromethyl)-1*H*-pyrazolo[3,4-*d*]pyrimidine **8d** (0.25 g, 0.69 mmol) in absolute ethanol (4 mL). The reaction mixture was irradiated in the microwave for

2–10 min at 80 °C in an open vessel. After cooling, the solvent was evaporated under reduced pressure, and the crude was treated with water (5 mL), then extracted with CH₂Cl₂ (5 mL); the organic phase was washed with water (5 mL), dried (MgSO₄), and concentrated under reduced pressure. The obtained oil was crystallized by adding a mixture of CH₂Cl₂/n-hexane (1:4) and standing in a refrigerator to afford the pure product as a white solid.

1-(2-Chloro-2-phenylethyl)-*N*-phenyl-6-(trifluoromethyl)-1*H*-pyrazolo[3,4-*d*]pyrimidin-4-amine **2k**. Yield: 65% (white solid). Mp: 139–141 °C. ¹H NMR (400 MHz, CDCl₃): δ 7.53–7.38 (m, 8H), 7.33–7.29 (m, 3H), 5.46–5.42 (m, 1H), 5.00–4.94 and 4.84–4.79 (2m, 2H). ¹³C NMR (101 MHz, CDCl₃): 155.95, 149.62, 141.42, 137.40, 133.90, 130.18, 129.90, 129.29, 128.87, 127.46, 123.84, 123.18, 110.63, 59.97, 54.15. IR (KBr disc) cm⁻¹: 3235 (NH). Elem. anal. calcd. For C₂₀H₁₅N₅ClF₃: C 57.49, H 3.92, N 16.76; found: C 57.44, H 4.15, N 16.43.

1-(2-Chloro-2-phenylethyl)-*N*-(3-fluorophenyl)-6-(trifluoromethyl)-1*H*-pyrazolo[3,4-*d*]pyrimidin-4-amine **2l**. Yield: 13% (white solid). Mp: 164–166 °C. ¹H NMR (400 MHz, CDCl₃): δ 8.63 (br s 1H), 7.51 (br s, 1H), 7.42–7.26 (m, 8H), 6.96 (t, 1H, *J* = 7.6 Hz), 5.51–5.48 (m, 1H), 5.02–4.97 and 4.87–4.82 (2m, 2H). ¹³C NMR (101 MHz, CDCl₃): δ 164.34, 161.88, 154.08, 139.30, 138.04, 137.59, 136.35, 135.48, 132.94, 132.69, 130.66, 130.57, 129.18, 128.82, 127.49, 127.48, 60.07, 54.06. IR (KBr disc) cm⁻¹: 3281 (NH). Elem. anal. calcd. For C₂₀H₁₄N₅ClF₄: C 55.12, H 3.24, N 16.07; found: C 55.36, H 3.34, N 15.89.

N-(3-Chlorophenyl)-1-(2-chloro-2-phenylethyl)-6-trifluoromethyl-1*H*-pyrazolo[3,4-*d*]pyrimidin-4-amine **2m**. Yield: 13% (white solid). Mp: 88–90 °C. ¹H NMR (400 MHz, CDCl₃): δ 8.18 (br s, 1H), 7.58 (br s, 1H), 7.43–7.39 (m, 5H), 7.34–7.28 (m, 4H), 5.49–5.45 (m, 1H), 5.03–4.97 and 4.87–4.82 (2m, 2H). NMR (101 MHz, CDCl₃): δ 147.88, 145.37, 137.41, 135.50, 134.72, 132.79, 130.89, 130.67, 129.48, 129.28, 128.90, 128.87, 127.91, 127.47, 127.45, 127.43, 59.98, 54.19. IR (KBr disc) cm⁻¹: 3308 (NH). Elem. anal. calcd. For C₂₀H₁₄N₅Cl₂F₃: C 53.11, H 3.12, N 15.49; found: C 53.12, H 3.15, N 15.46.

3.1.4. General Procedure for the Synthesis of Intermediates **5a,b**

Ethoxymethylenemalononitrile (2.44 g, 20 mmol) was added to a solution of the opportune 2-hydrazino-1-phenylethanol **4a,b** (20 mmol) in absolute ethanol (40 mL) and the reaction mixture was refluxed for 6 h. The solvent was concentrated to 50% of the initial volume and cooled. The yellow solid obtained was filtered and recrystallized from absolute ethanol.

5-Amino-1-(2-hydroxy-2-phenylethyl)-1*H*-pyrazole-4-carbonitrile **5a**. Yield: 71% (white solid). Analytical and spectroscopic data are in accordance with those previously reported by us [20].

5-Amino-1-[2-(4-chlorophenyl)-2-hydroxyethyl]-1*H*-pyrazole-4-carbonitrile **5b**. Yield: 51% (white solid). Mp: 218–220 °C. ¹H NMR (400 MHz, DMSO-*d*₆): δ 7.50 (s, 1H), 7.36–7.31 (m, 4H), 6.41 (br s, 2H), 5.72 (d, 1H, *J* = 4.8 Hz), 4.92–4.88 (m, 1H), 4.05–4.00 and 3.95–3.90 (2m, 2H). ¹³C NMR (101 MHz, DMSO-*d*₆): δ 152.62, 141.93, 140.63, 132.43, 128.69, 128.54, 115.86, 72.63, 71.01, 54.37. IR (KBr disc) cm⁻¹: 3401–3287 (OH, NH₂), 2217 (CN). Elem. anal. calcd. For C₁₂H₁₁N₄ClO: C 54.87, H 4.22, N 21.33; found: C 55.01, H 4.23, N 21.42.

3.1.5. General Procedure for the Synthesis of Intermediates **6a,b**

2M NaOH (10 mL) was added to a solution of the opportune 5-amino-1-(2-hydroxy-2-phenylethyl)-1*H*-pyrazole-4-carboxamide derivative **5a,b** (10 mmol) in absolute ethanol (10 mL), and the mixture was refluxed for 2 h. After cooling, the solid obtained was filtered, washed with water and recrystallized from ethanol.

5-Amino-1-(2-hydroxy-2-phenylethyl)-1*H*-pyrazole-4-carboxamide **6a**. Yield: 66% (white solid). Analytical and spectroscopic data are in accordance with those previously reported by us [20].

5-Amino-1-[2-(4-chloro-phenyl)-2-hydroxyethyl]-1*H*-pyrazole-4-carboxamide **6b**. Yield: 58% (white solid). Mp: 215–216 °C. ¹H NMR (400 MHz, DMSO-*d*₆): δ 7.59 (s, 1H),

7.36–7.31 (m, 4H), 6.05 (br s, 2H), 5.79 (br s, 1H), 4.93–4.90 (m, 1H), 4.00–3.89 (m, 2H). IR (KBr disc) cm^{-1} : 3450–3200 (OH + NH), 1622 (CO). ^{13}C NMR (101 MHz, DMSO- d_6): δ 166.67, 150.51, 142.20, 137.67, 132.31, 128.62, 128.53, 97.27, 71.31, 54.16. Elem. anal. calcd. For $\text{C}_{12}\text{H}_{13}\text{N}_4\text{O}_2\text{Cl}$: C 51.34, H 4.67, N 19.96; found: C 51.41, H 4.87, N 19.98.

3.1.6. General Procedure for the Synthesis of 6-Substituted 1-(2-Hydroxy-2-Phenylethyl)-1,5-Dihydro-4H-Pyrazolo[3,4-*d*]Pyrimidin-4-one Derivatives 7a-h

A solution of sodium ethoxide prepared from sodium (1.38 g, 60 mmol) and absolute ethanol (30 mL) and the appropriate alkyl ester (60 mmol) were added to a solution of the appropriate 5-amino-1-(2-hydroxy-2-phenylethyl)-1H-pyrazole-4-carboxamide 6a,b (10 mmol) in absolute ethanol (90 mL). The mixture was refluxed for 6–12 h; after cooling, ice water was added, and the solution was acidified with 3% acetic acid. The obtained precipitate was filtered, washed with water, and recrystallized from absolute ethanol to afford desired compounds 7a-h.

6-Ethyl-1-(2-hydroxy-2-phenylethyl)-1,5-dihydro-4H-pyrazolo[3,4-*d*]pyrimidin-4-one **7a**. Alkyl ester used for the synthesis: methyl propionate. Yield: 65% (white solid). Mp: 221–222 °C. ^1H NMR (400 MHz, DMSO- d_6): δ 11.90 (br s, 1H), 7.94 (s, 1H), 7.26–7.21 (m, 4H), 7.20–7.16 (m, 1H), 5.59 (br s, 1H), 5.05 (br s, 1H), 4.42–4.37 and 4.28–4.23 (2m, 2H), 2.54 (q, 2H, $J = 7.6$ Hz), 1.14 (t, 3H, $J = 7.6$ Hz). ^{13}C NMR (101 MHz, DMSO- d_6): δ 161.85, 158.59, 153.39, 143.01, 134.53, 128.55, 127.89, 126.54, 104.27, 71.66, 54.48, 28.00, 11.87. IR (KBr disc) cm^{-1} : 3410 (NH), 3350–2990 (OH), 1661 (CO). Elem. anal. calcd. for $\text{C}_{15}\text{H}_{16}\text{N}_4\text{O}_2$: C 63.37, H 5.67, N 19.71; found: C 63.15, H 5.91, N 19.59.

6-Cyclopentyl-1-(2-hydroxy-2-phenylethyl)-1,5-dihydro-4H-pyrazolo[3,4-*d*]pyrimidin-4-one **7b**. Alkyl ester used for the synthesis: methyl cyclopentancarboxylate. Yield: 44% (white solid). Mp: 227–228 °C. ^1H NMR (200 MHz, CDCl_3): δ 10.95 (br s, 1H), 7.99 (s, 1H), 7.34–7.32, 7.29–7.25 and 7.22–7.17 (3m, 5H), 5.16–5.14 (m, 1H), 4.61–4.56 and 4.50–4.44 (2m, 2H), 4.33 (br s, 1H), 3.04 (t, 1H, $J = 7.0$ Hz), 2.06–2.04 (m, 2H), 1.88–1.1.79 (m, 4H), 1.71–1.66 (m, 2H). IR (KBr disc) cm^{-1} : 3300–2950 (NH + OH), 1698 (CO). Elem. anal. calcd. for $\text{C}_{18}\text{H}_{20}\text{N}_4\text{O}_2$: C 66.65, H 6.21, N 17.27; found: C 66.84, H 6.29, N 17.31.

6-Cyclohexyl-1-(2-hydroxy-2-phenylethyl)-1,5-dihydro-4H-pyrazolo[3,4-*d*]pyrimidin-4-one **7c**. Alkyl ester used for the synthesis: methyl cyclohexane carboxylate. Yield: 68% (white solid). Mp: 216–218 °C. ^1H NMR (400 MHz, DMSO- d_6): δ 7.92 (s, 1H), 7.24–7.16 (m, 5H), 5.64 (br s, 1H), 5.07–5.03 (m, 1H), 4.42–4.36 and 4.31–4.26 (2m, 2H), 2.55–2.50 (m, 1H), 1.80–1.62 (m, 4H), 1.66–1.62 (m, 1H), 1.52–1.39 (m, 2H), and 1.29–1.13 (m, 3H). ^{13}C NMR (101 MHz, DMSO- d_6): δ 164.31, 158.78, 153.31, 142.97, 134.46, 128.50, 127.86, 126.54, 104.35, 71.68, 54.43, 42.83, 30.73, 30.69, 25.87, 25.81. IR (KBr disc) cm^{-1} : 3330–3000 (NH + OH), 1701 (CO). Elem. anal. calcd. for $\text{C}_{19}\text{H}_{22}\text{N}_4\text{O}_2$: C 67.44, H 6.55, N 16.56; found C 67.58, H 8.82, N 16.44.

1-(2-Hydroxy-2-phenylethyl)-6-(trifluoromethyl)-1,5-dihydro-4H-pyrazolo[3,4-*d*]pyrimidin-4-one **7d**. Alkyl ester used for the synthesis: methyl trifluoroacetate. Yield: 58% (white solid). Mp: 212–214 °C. ^1H NMR (200 MHz, DMSO- d_6): δ 13.58 (br s, 1H), 8.23 (s, 1H), 7.38–7.19 (m, 5H), 5.71 (d, 1H, $J = 6.1$ Hz), 5.13–5.06 (m, 1H), 4.58–4.27 (m, 2H). IR (KBr disc) cm^{-1} : 3450–2798 (OH + NH), 1704 (CO). Elem. anal. calcd. for $\text{C}_{14}\text{H}_{11}\text{N}_4\text{O}_2\text{F}_3$: C 51.86, H 3.42, N 17.58; found: C 51.78, H 3.77, N 17.34.

1-(2-Hydroxy-2-phenylethyl)-6-phenyl-1,5-dihydro-4H-pyrazolo[3,4-*d*]pyrimidin-4-one **7e**. Alkyl ester used for the synthesis: methyl benzoate. Yield: 53% (white solid). Mp: 252–254 °C. ^1H NMR (200 MHz, DMSO- d_6): δ 12.36 (br s, 1H), 8.12–8.11, 7.60–7.58 and 7.34–7.31 (3m, 11H), 5.61 (d, 1H, $J = 4.7$ Hz), 5.18–5.06 (m, 1H), 4.61–4.28 (m, 2H). IR (KBr disc) cm^{-1} : 3445–2977 (OH + NH), 1695 (CO). Elem. anal. calcd. for $\text{C}_{19}\text{H}_{16}\text{N}_4\text{O}_2$: C 68.66, H 4.85, N 16.86; found: C 68.38, H 5.09, N 17.02.

1-[2-(4-Chlorophenyl)-2-hydroxyethyl]-6-methyl-1,5-dihydro-4H-pyrazolo[3,4-*d*]pyrimidin-4-one **7f**. Alkyl ester used for the synthesis: ethyl acetate. Yield: 72% (white solid). Mp: 264–266 °C. ^1H NMR (200 MHz, DMSO- d_6): δ 8.00 (s, 1H), 7.39–7.27 (m, 4H), 5.75 (d, 1H, $J = 4.8$ Hz), 5.17–5.04 (m, 1H), 4.43–4.39 and 4.30–4.19 (2m, 2H), 2.33 (s, 3H). IR (KBr disc)

cm⁻¹: 3230–2950 (NH + OH), 1677 (CO). Elem. anal. calcd. for C₁₄H₁₃N₄ClO₂: C 55.18, H 4.30, N 18.39; found: C 55.26, H 4.59, N 18.26.

1-[2-(4-Chlorophenyl)-2-hydroxyethyl]-6-ethyl-1,5-dihydro-4*H*-pyrazolo[3,4-*d*]pyrimidin-4-one **7g**. Alkyl ester used for the synthesis: methyl propionate. Yield: 71% (white solid). Mp: 243–245 °C. ¹H NMR (200 MHz, DMSO-*d*₆): δ 12.10 (br s, 1H), 8.14 (s, 1H), 7.48–7.35 (m, 4H), 5.39 (br s, 1H), 5.23–5.19 (m, 1H), 4.64–4.41 (m, 2H), 2.71 (q, 2H, *J* = 7.8 Hz), 1.31 (t, 3H, *J* = 7.8 Hz). IR (KBr disc) cm⁻¹: 3400–2900 (OH + NH), 1693 (CO). Elem. anal. calcd. for C₁₅H₁₅N₄ClO₂: C 56.52, H 4.74, N 17.58; found: C 56.78, H 4.94; N 17.60.

1-[2-(4-Chlorophenyl)-2-hydroxyethyl]-6-propyl-1,5-dihydro-4*H*-pyrazolo[3,4-*d*]pyrimidin-4-one **7h**. Alkyl ester used for the synthesis: methyl butyrate. Yield: 80% (white solid). Mp: 257–259 °C. ¹H NMR (200 MHz, DMSO-*d*₆): δ 8.00 (s, 1H), 7.34–7.18 (m, 4H), 5.80 (d, 1H, *J* = 4.6 Hz), 5.17–5.03 (m, 1H), 4.43–4.21 (m, 2H), 1.65 (sx, 2H, *J* = 7.4 Hz), 0.88 (t, 3H, *J* = 7.4 Hz). IR (KBr disc) cm⁻¹: 3440–2900 (NH + OH), 1694 (CO). Elem. anal. calcd. for C₁₆H₁₇N₄O₂Cl: C 57.75, H 5.15, N 16.84; found: C 58.07, H 5.48; N 16.98.

3.1.7. General Procedure for the Synthesis of 6-Alkyl or 6-Phenyl 4-Chloro-1-(2-Chloro-2-Phenylethyl)-1*H*-Pyrazolo[3,4-*d*]pyrimidines **8a-h**

The Vilsmeier complex, previously prepared from POCl₃ (4.60 g, 30 mmol) and anhydrous DMF (2.20 g, 30 mmol), was added to a suspension of the appropriate intermediate **7a-h** (1 mmol) in CHCl₃ (10 mL). The mixture was refluxed for 6–12 h. The solution was washed with water (2 × 20 mL), dried (MgSO₄), filtered, and concentrated under reduced pressure. The crude oil was purified by column chromatography (Florisil, 100–200 mesh), using diethyl ether as eluant, to afford compounds **8a-c**, **f-h** as yellow or colorless oils. Compounds **8d,e** crystallized standing in a refrigerator by adding a 1:1 mixture of diethyl ether/petroleum ether (bp 40–60 °C) (1:1) as white solids.

4-Chloro-1-(2-chloro-2-phenylethyl)-6-ethyl-1*H*-pyrazolo[3,4-*d*]pyrimidine **8a**. Yield: 85% (colorless oil). ¹H NMR (400 MHz, CDCl₃): δ 11.29 (br s, 1H), 8.05 (s, 1H), 7.40–7.37 (m, 2H), 7.32–7.25 (m, 3H), 5.49–5.46 (m, 1H), 4.92–4.86 and 4.78–4.72 (2m, 2H), 2.74 (q, 2H, *J* = 7.2 Hz), 1.35 (t, 3H, *J* = 7.2 Hz). ¹³C NMR (101 MHz, CDCl₃): 161.18, 160.03, 153.79, 137.86, 135.47, 129.04, 128.75, 127.47, 103.99, 60.19, 54.01, 28.56, 11.29. Elem. anal. calcd. for C₁₅H₁₄N₄Cl₂: C 56.09, H 4.39, N 17.44; found: C 56.18, H 4.51, N 17.63.

4-Chloro-1-(2-chloro-2-phenylethyl)-6-cyclopentyl-1*H*-pyrazolo[3,4-*d*]pyrimidine **8b**. Yield: 95% (yellow oil). ¹H NMR (200 MHz, CDCl₃): δ 8.04 (s, 1H), 7.39–7.24 (m, 5H), 5.28–5.21 (m, 1H), 4.67–4.59 and 4.54–4.43 (2m, 2H), 3.12–3.02 (m, 1H), 1.87–1.43 (m, 8H). Elem. anal. calcd. for C₁₈H₁₈N₄Cl₂: C 58.84, H 5.02, N 15.51; found: C 60.00, H 4.99, N 15.21.

4-Chloro-1-(2-chloro-2-phenylethyl)-6-cyclohexyl-1*H*-pyrazolo[3,4-*d*]pyrimidine **8c**. Yield: 98% (yellow oil). ¹H NMR (200 MHz, DMSO-*d*₆): δ 8.45 (s, 1H), 7.48–7.42 and 7.35–7.33 (2m, 5H), 5.78–5.67 (m, 1H), 5.15–4.96 (m, 2H), 2.88 (t, 1H, *J* = 7.8 Hz), 2.00–1.94 and 1.94–1.33 (2m, 10H). Elem. anal. calcd. for C₁₉H₂₀N₄Cl₂: C 60.81, H 5.37, N 14.93; found: C 60.96, H 5.44, N 15.03.

4-Chloro-1-(2-chloro-2-phenylethyl)-6-(trifluoromethyl)-1*H*-pyrazolo[3,4-*d*]pyrimidine **8d**. Yield: 84% (white solid). ¹H NMR (200 MHz, DMSO-*d*₆): δ 8.08 (s, 1H), 7.52–7.50 and 7.40–7.35 (2m, 5H), 5.77–5.65 (m, 1H), 5.23–4.98 (m, 2H). Mp: 85–87 °C. Elem. anal. calcd. for C₁₄H₉N₄Cl₂F₃: C 46.56, H 2.51, N 15.51; found: 46.78, H 2.80, N 15.20.

4-Chloro-1-(2-chloro-2-phenylethyl)-6-phenyl-1*H*-pyrazolo[3,4-*d*]pyrimidine **8e**. Yield: 81% (white solid). Mp: 114–117 °C. ¹H NMR (200 MHz, CDCl₃): δ 8.59–8.56 (m, 2H), 8.16–8.14 (m, 1H), 7.59–7.51 (m, 5H), 7.48–7.31 (m, 3H), 5.63–5.59 (m, 1H), 5.21–4.98 (m, 2H). Elem. anal. calcd. for C₁₉H₁₄N₄Cl₂: C 61.80, H 3.82, N 15.17; found: C 61.74, H 4.03, N 14.83.

4-Chloro-1-[2-chloro-2-(4-chlorophenyl)ethyl]-6-methyl-1*H*-pyrazolo[3,4-*d*]pyrimidine **8f**. Yield: 94% (colorless oil). ¹H NMR (200 MHz, CDCl₃): δ 7.97 (s, 1H), 7.38–7.29 (m, 4H), 5.58–5.50 (m, 1H), 5.18–5.00 and 4.95–4.79 (2m, 2H), 2.70 (s, 3H). Elem. anal. calcd. for C₁₄H₁₁N₄Cl₃: C 49.22, H 3.25, N 16.40; found: C 49.13, H 2.98, N 16.31.

4-Chloro-1-[2-chloro-2-(4-chloro-phenyl)-ethyl]-6-ethyl-1*H*-pyrazolo[3,4-*d*]pyrimidine **8g**. Yield: 81% (yellow oil, that slowly crystallized). Mp: 63–65 °C. ¹H NMR (200 MHz,

DMSO- d_6): δ 8.46 (s, 1H), 7.55–7.51 and 7.46–7.39 (2m, 4H), 5.78–5.66 (m, 1H), 5.17–4.92 (m, 2H), 2.96 (q, 2H, $J = 7.6$ Hz), 1.31 (t, 3H, $J = 7.6$ Hz). Elem. anal. calcd. for $C_{15}H_{13}N_4Cl_3$: C 50.66, H 3.68, N 15.75; found C 50.47, H 3.50, N 15.60.

4-Chloro-1-[2-chloro-2-(4-chlorophenyl)ethyl]-6-propyl-1H-pyrazolo[3,4-*d*]pyrimidine **8h**. Yield: 93% (yellow oil). 1H NMR (200 MHz, DMSO- d_6): δ 7.90 (s, 1H), 7.58–7.39 (m, 4H), 5.44–5.38 (m, 1H), 5.09–5.01 (m, 2H), 2.65 (t, $J = 7.7$ Hz, 2H), 1.80 (sx, 2H, $J = 7.7$ Hz), 0.89 (t, 3H, $J = 7.7$ Hz). Elem. anal. calcd. for $C_{16}H_{15}N_4Cl_3$: C 51.98, H 4.09, N 15.16; found: C 52.20, H 4.17, N 15.21.

3.2. Enzymatic Assay

Src, Fyn, and Abl were purchased from Merck-Millipore. Reactions were performed according to the manufacturer's instructions with minor modifications. All substrates were used at least at twice the concentration of apparent K_m . In detail: Src reactions were performed using 500 μM Src-peptide (KVEKIGEGTYGVVYK), 100 μM ATP, and 0.00087% NP-40; Fyn reactions were performed using 360 μM Src-peptide (KVEKIGEGTYGVVYK), 200 μM ATP, and 0.0026% NP-40; Abl reactions were performed using 50 μM abltide (EAIYAAPFAKKK), 30 μM ATP, and 0.00087% NP-40. All reactions were performed using 10–50 ng of enzyme and 10% DMSO in 10 μL of kinase buffer (8 mM MOPS-NaOH pH7.0, 0.2 mM EDTA, 10 mM MgAc) at 30 $^\circ C$ for 10 min.

To avoid peptide adsorbing to the plastic surface, protein low-binding tubes were used. ADP-Glo kinase assay (Promega) was then used to detect kinase activity according to the manufacturer's instructions with minor modifications. In detail, reactions were transferred to white 384 well-plates and stopped by adding 10 μL of ADP-Glo reagent (Promega) for 50 min at room temperature. A total of 20 μL of detection reagent (Promega) was then added for 30 min and the reaction read using a GloMax Discover microplate reader (Promega). Data were plotted using GraphPad Prism 5.0. IC_{50} values were obtained according to Equation (1):

$$v = V / \{1 + (I/IC_{50})\} \quad (1)$$

where v is the measured reaction velocity, V is the apparent maximal velocity in the absence of inhibitor, I is the inhibitor concentration, and IC_{50} is the 50% inhibitory dose. Compounds tested were assumed to act as fully ATP-competitive inhibitors. Therefore, K_i values were calculated according to Equation (2):

$$K_i = IC_{50} / (1 + K_m / [S]) \quad (2)$$

where K_i is the affinity of the inhibitor to the enzyme, S is the ATP concentration, and K_m is the affinity of ATP calculated according to the Michaelis–Menten equation.

3.3. Cell Biology

3.3.1. Cell Culture

All glioblastoma cell lines were cultured as previously described [21]. In more detail, T98G (Elabscience) and U251 cells were cultured in DMEM supplemented with 10% fetal bovine serum and routinely tested negative for mycoplasma contamination. GBMSC83 cells, a well-characterized mesenchymal GBM cancer stem cellular model, were cultured in non-adherent conditions as 3D neurospheres in DMEM-F12 supplemented with B27 Supplement (50 \times), EGF (20 ng/mL), and h β FGF(10 ng/mL) as previously described in [22,23].

3.3.2. Antibodies and Other Reagents

Anti-GAPDH (Santa Cruz 1:5000, D16H11); anti-Vinculin (Cell signaling 1:5000, 13901T); anti-Src (Cell signaling 1:1000, 2108S); anti-pY416-Src (Cell signaling 1:1000, 2101S).

Dasatinib (Sigma Aldrich, DAS, Merck Millipore, Burlington, MA, USA), SI388 and SI83 were used at different concentration (10 nM, 1 μM or 25 μM) for 24 h upon serum deprivation. DMSO (Sigma Aldrich) was used as the control.

3.3.3. Protein Extracts and Immunoblotting Analysis

Cell extracts were prepared in RIPA (50 mM Tris-HCl pH 8.0, 150 mM NaCl, 1% NP40, 1 mM EGTA, 1 mM EDTA, 0.25% sodium deoxycholate) or IP buffer (50 mM Tris-HCl pH 7.5, 250 mM NaCl, 1% NP-40, 5 mM EDTA, 5 mM EGTA) supplemented with protease and phosphatase inhibitors (Roche Diagnostic, Mannheim, Germany). For immunoblotting, 25–30 µg of protein was separated by sodium dodecyl sulfate (SDS) polyacrylamide gel electrophoresis (PAGE), blotted onto nitrocellulose membrane, and detected with specific antibodies.

3.3.4. Clonogenic Survival Assay

For colony formation, control and irradiated (5 Gy) cells were seeded at the concentration of 1000 cells/dish in 6-well culture plates and incubated at 37 °C, 5% CO₂ for 10–15 days.

Crystal violet solution (10% (v/v) methanol and 0.5% Crystal Violet) was used to fix and stain colonies, upon 20 min incubation. The stained colonies (>50 cells) were counted under a microscope or using Image “Colonyarea” plugin. Data were expressed as the mean and SD of three independent experiments.

3.3.5. MTS Assay

Cells were plated in 96 multiwells (1000 cells/well) in 100 µL of the complete medium. The following day, after 24 h of starvation, the cells were treated with DMSO, dasatinib or SI388 at different concentrations (10 nM, 1 µM, 25 µM). After 72 h, cells were treated with tetrazolium (Promega) for 1–2 h. The quantity of formazan product is directly proportional to the number of living cells in the culture. The plate is then read with a plate reader measuring the absorbance of 490 nm for the different conditions.

3.3.6. Neurosphere Formation, Cell Counting and Sphere Size Measurement

GBMSC83 cells were seeded at the density of 1×10^4 cells/well in a 96-well ultralow attachment plate, and the following day they were treated with SI388 1 µM or dasatinib 1 µM. After 72 h from treatment, cells were stained with Hoechst 33,342 (Thermo Fisher Scientific) and images were acquired with Fluorescence microscopy (ZEISS) and processed with Fiji version 2.3. Hoechst positive nuclei were counted by particle detection instrument of ComDet Plugin of Fiji. The bright fields were acquired and processed by Cell Profiler version 2.1.1 to measure spheres' diameter and reported as the fold change from the control condition.

3.3.7. Cell Death Analysis

1×10^6 cells were analyzed for cell death 48 h from ionizing radiation (10 Gy) upon staining with Annexin V-APC-propidium iodide (PI) kit, according to manufacturer instructions (eBioscience™ Annexin V apoptosis detection kits, ThermoFisher Scientific, Waltham, MA, USA). Unstained samples were used as the control. CytoFLEX S (Beckman Coulter, Milan, Italy) instrument was used to quantify the double staining. Quality control was evaluated using CytoFLEX Daily QC Fluorospheres (Beckman Coulter). CytExpert version 2.2 software (Beckman Coulter) was used to analyze FCS files. Dead cells were graphed as fold change to control conditions.

3.3.8. Statistical Analyses

All data were analyzed and presented as mean ± S.E.M. The significance of the differences between populations of data were assessed according to the paired or unpaired Student's two-tailed *t*-test with a level of significance of at least $p \leq 0.05$.

4. Conclusions

We performed a lead optimization study that afforded the discovery of the compound SI388 (2a), endowed with an improved activity compared to the parent compound SI83

(1a). This promising cell-free data prompted us to investigate the efficacy of SI388 in 2D and 3D tumor models characterized by Src overexpression. For this purpose, we decided to perform our biological experiments using GBM cellular models, which are known to be characterized by Src hyperactivation.

In this work, we tested SI388 compound on two commercial GBM cell lines (T98G and U251 cells) and on mesenchymal patient-derived cancer stem cells (GBMSC83 cells). Interestingly, SI388 can efficiently target Src and its functionality both in T98G and U251 cell lines as well as in GBMSC83 patient-derived neurospheres. Importantly, SI388 can sensitize patient derived GBM cells to IR treatment, similarly to dasatinib. Overall, this study identifies SI388 as a promising candidate for Src kinase inhibition and as a potential new tool to enhance responses to radiotherapy, which is worthy of further investigation.

Supplementary Materials: The following supporting information can be downloaded at: <https://www.mdpi.com/article/10.3390/ph16070958/s1>. Table S1: Percentage of Src inhibition at 100, 10 and 1 μ M for compounds 2a-s.

Author Contributions: Conceptualization, F.M., S.S. and D.B.; writing—original draft preparation, A.C. (Anna Carbone), E.C., C.P., F.M., D.B., C.C. (Claudia Contadini) and C.C. (Claudia Cirotti); review and editing, A.C. (Annarita Ciancusi), F.M., S.S., G.M., C.C. (Claudia Contadini), C.C. (Claudia Cirotti) and D.B.; in-vestigation, C.C. (Claudia Contadini), C.C. (Claudia Cirotti), E.C., C.P., F.M. and M.N.; data cura-tion, C.C. (Claudia Contadini), C.C. (Claudia Cirotti), E.C. and F.M. All authors have read and agreed to the published version of the manuscript.

Funding: This work has been supported by the Associazione Italiana per la Ricerca sul Cancro AIRC-IG2021 n.26230 (D.B.), IG2017 n.20702 (G.M.), IG2020 n.24448 (E.C.), IG2019, n. 23725 (S.S.); the Italian Ministry of Health, RF-2016-02362022 (D.B.); the MIUR Project PRIN 2017 2017SA5837_004 (G.M. S.S., F.M., and C.P.); the Cariplo Foundation, project 2019-1836 (E.C.); C.Co.'s work has also been supported by AIRC-IG2021-n.26230, C.Ci has been supported by a the FIRC-AIRC fellowship for Italy "Filomena Todini".

Institutional Review Board Statement: Not applicable.

Informed Consent Statement: Not applicable.

Data Availability Statement: Data is contained within the article and Supplementary Material.

Acknowledgments: We thank Maria Pia Gentileschi for kindly providing technical support for irradiation experiments.

Conflicts of Interest: The authors declare that they have no known competing financial interests or personal relationships that could have appeared to influence the work reported in this paper.

References

1. Sefton, B.M.; Hunter, T.; Beemon, K. Product of in Vitro Translation of the Rous Sarcoma Virus Src Gene Has Protein Kinase Activity. *J. Virol.* **1979**, *30*, 311–318. [[CrossRef](#)]
2. Stehelin, D.; Varmus, H.E.; Bishop, J.M.; Vogt, P.K. DNA Related to the Transforming Gene(s) of Avian Sarcoma Viruses Is Present in Normal Avian DNA. *Nature* **1976**, *260*, 170–173. [[CrossRef](#)]
3. Martin, G.S. Rous Sarcoma Virus: A Function Required for the Maintenance of the Transformed State. *Nature* **1970**, *227*, 1021–1023. [[CrossRef](#)] [[PubMed](#)]
4. Cirotti, C.; Contadini, C.; Barilà, D. SRC Kinase in Glioblastoma: News from an Old Acquaintance. *Cancers* **2020**, *12*, 1558. [[CrossRef](#)] [[PubMed](#)]
5. Radi, M.; Tintori, C.; Musumeci, F.; Brullo, C.; Zamperini, C.; Dreassi, E.; Fallacara, A.L.; Vignaroli, G.; Crespan, E.; Zanolì, S.; et al. Design, Synthesis, and Biological Evaluation of Pyrazolo[3,4-d]Pyrimidines Active in Vivo on the Bcr-Abl T315I Mutant. *J. Med. Chem.* **2013**, *56*, 5382–5394. [[CrossRef](#)] [[PubMed](#)]
6. Vignaroli, G.; Iovenitti, G.; Zamperini, C.; Coniglio, F.; Calandro, P.; Molinari, A.; Fallacara, A.L.; Sartucci, A.; Calgani, A.; Colecchia, D.; et al. Prodrugs of Pyrazolo[3,4-d]Pyrimidines: From Library Synthesis to Evaluation as Potential Anticancer Agents in an Orthotopic Glioblastoma Model. *J. Med. Chem.* **2017**, *60*, 6305–6320. [[CrossRef](#)]
7. Tintori, C.; Fallacara, A.L.; Radi, M.; Zamperini, C.; Dreassi, E.; Crespan, E.; Maga, G.; Schenone, S.; Musumeci, F.; Brullo, C.; et al. Combining X-Ray Crystallography and Molecular Modeling toward the Optimization of Pyrazolo[3,4-d]Pyrimidines as Potent c-Src Inhibitors Active in Vivo against Neuroblastoma. *J. Med. Chem.* **2015**, *58*, 347–361. [[CrossRef](#)]

8. Radi, M.; Dreassi, E.; Brullo, C.; Crespan, E.; Tintori, C.; Bernardo, V.; Valoti, M.; Zamperini, C.; Daigl, H.; Musumeci, F.; et al. Design, Synthesis, Biological Activity, and ADME Properties of Pyrazolo[3,4-d]Pyrimidines Active in Hypoxic Human Leukemia Cells: A Lead Optimization Study. *J. Med. Chem.* **2011**, *54*, 2610–2626. [[CrossRef](#)]
9. Manetti, F.; Santucci, A.; Locatelli, G.A.; Maga, G.; Spreafico, A.; Serchi, T.; Orlandini, M.; Bernardini, G.; Caradonna, N.P.; Spallarossa, A.; et al. Identification of a Novel Pyrazolo[3,4-d]Pyrimidine Able To Inhibit Cell Proliferation of a Human Osteogenic Sarcoma in Vitro and in a Xenograft Model in Mice. *J. Med. Chem.* **2007**, *50*, 5579–5588. [[CrossRef](#)]
10. Ahluwalia, M.S.; de Groot, J.; Liu, W.M.; Gladson, C.L. Targeting SRC in Glioblastoma Tumors and Brain Metastases: Rationale and Preclinical Studies. *Cancer Lett.* **2010**, *298*, 139–149. [[CrossRef](#)]
11. Contadini, C.; Ferri, A.; Di Martile, M.; Cirotti, C.; Del Bufalo, D.; De Nicola, F.; Pallocca, M.; Fanciulli, M.; Sacco, F.; Donninelli, G.; et al. Caspase-8 as a Novel Mediator Linking Src Kinase Signaling to Enhanced Glioblastoma Malignancy. *Cell Death Differ.* **2023**, *30*, 417–428. [[CrossRef](#)]
12. Di Maria, S.; Picarazzi, F.; Mori, M.; Ciancusi, A.; Carbone, A.; Crespan, E.; Perini, C.; Sabetta, S.; Deplano, S.; Poggialini, F.; et al. Novel Pyrazolo[3,4-d]Pyrimidines as Dual Src/Bcr-Abl Kinase Inhibitors: Synthesis and Biological Evaluation for Chronic Myeloid Leukemia Treatment. *Bioorg. Chem.* **2022**, *128*, 106071. [[CrossRef](#)] [[PubMed](#)]
13. Molinari, A.; Fallacara, A.L.; Di Maria, S.; Zamperini, C.; Poggialini, F.; Musumeci, F.; Schenone, S.; Angelucci, A.; Colapietro, A.; Crespan, E.; et al. Efficient Optimization of Pyrazolo[3,4-d]Pyrimidines Derivatives as c-Src Kinase Inhibitors in Neuroblastoma Treatment. *Bioorg. Med. Chem. Lett.* **2018**, *28*, 3454–3457. [[CrossRef](#)] [[PubMed](#)]
14. Kruewel, T.; Schenone, S.; Radi, M.; Maga, G.; Rohrbeck, A.; Botta, M.; Borlak, J. Molecular Characterization of C-Abl/c-Src Kinase Inhibitors Targeted against Murine Tumour Progenitor Cells That Express Stem Cell Markers. *PLoS ONE* **2010**, *5*, e14143. [[CrossRef](#)] [[PubMed](#)]
15. Carraro, F.; Naldini, A.; Pucci, A.; Locatelli, G.A.; Maga, G.; Schenone, S.; Bruno, O.; Ranise, A.; Bondavalli, F.; Brullo, C.; et al. Pyrazolo[3,4-d]Pyrimidines as Potent Antiproliferative and Proapoptotic Agents toward A431 and 8701-BC Cells in Culture via Inhibition of c-Src Phosphorylation. *J. Med. Chem.* **2006**, *49*, 1549–1561. [[CrossRef](#)]
16. Radi, M.; Brullo, C.; Crespan, E.; Tintori, C.; Musumeci, F.; Biava, M.; Schenone, S.; Dreassi, E.; Zamperini, C.; Maga, G.; et al. Identification of Potent C-Src Inhibitors Strongly Affecting the Proliferation of Human Neuroblastoma Cells. *Bioorg. Med. Chem. Lett.* **2011**, *21*, 5928–5933. [[CrossRef](#)]
17. Cancer Genome Atlas Research Network Comprehensive Genomic Characterization Defines Human Glioblastoma Genes and Core Pathways. *Nature* **2008**, *455*, 1061–1068. [[CrossRef](#)]
18. Verhaak, R.G.W.; Hoadley, K.A.; Purdom, E.; Wang, V.; Qi, Y.; Wilkerson, M.D.; Miller, C.R.; Ding, L.; Golub, T.; Mesirov, J.P.; et al. Integrated Genomic Analysis Identifies Clinically Relevant Subtypes of Glioblastoma Characterized by Abnormalities in PDGFRA, IDH1, EGFR, and NF1. *Cancer Cell* **2010**, *17*, 98–110. [[CrossRef](#)]
19. Alhalabi, O.T.; Fletcher, M.N.C.; Hielscher, T.; Kessler, T.; Lokumcu, T.; Baumgartner, U.; Wittmann, E.; Schlue, S.; Göttmann, M.; Rahman, S.; et al. A Novel Patient Stratification Strategy to Enhance the Therapeutic Efficacy of Dasatinib in Glioblastoma. *Neuro Oncol.* **2022**, *24*, 39–51. [[CrossRef](#)]
20. Greco, C.; Catania, R.; Balacco, D.L.; Taresco, V.; Musumeci, F.; Alexander, C.; Huett, A.; Schenone, S. Synthesis and Antibacterial Evaluation of New Pyrazolo[3,4-d]Pyrimidines Kinase Inhibitors. *Molecules* **2020**, *25*, 5354. [[CrossRef](#)]
21. Fianco, G.; Mongiardi, M.P.; Levi, A.; De Luca, T.; Desideri, M.; Trisciuglio, D.; Bufalo, D.D.; Cinà, I.; Benedetto, A.D.; Mottolese, M.; et al. Caspase-8 Contributes to Angiogenesis and Chemotherapy Resistance in Glioblastoma. *Elife* **2017**, *6*, 1–16. [[CrossRef](#)] [[PubMed](#)]
22. Minata, M.; Audia, A.; Shi, J.; Lu, S.; Bernstock, J.; Pavlyukov, M.S.; Das, A.; Kim, S.-H.; Shin, Y.J.; Lee, Y.; et al. Phenotypic Plasticity of Invasive Edge Glioma Stem-like Cells in Response to Ionizing Radiation. *Cell Rep.* **2019**, *26*, 1893–1905.e7. [[CrossRef](#)] [[PubMed](#)]
23. Mao, P.; Joshi, K.; Li, J.; Kim, S.-H.; Li, P.; Santana-Santos, L.; Luthra, S.; Chandran, U.R.; Benos, P.V.; Smith, L.; et al. Mesenchymal Glioma Stem Cells Are Maintained by Activated Glycolytic Metabolism Involving Aldehyde Dehydrogenase 1A3. *Proc. Natl. Acad. Sci. USA* **2013**, *110*, 8644–8649. [[CrossRef](#)] [[PubMed](#)]

Disclaimer/Publisher's Note: The statements, opinions and data contained in all publications are solely those of the individual author(s) and contributor(s) and not of MDPI and/or the editor(s). MDPI and/or the editor(s) disclaim responsibility for any injury to people or property resulting from any ideas, methods, instructions or products referred to in the content.